

Ion Solvation via Neutron Scattering

John E. Enderby

H. H. Wills Physics Laboratory, University of Bristol, Bristol BS8 1TL, U.K.

1 Introduction

The recognition that the hydration of ions has a major role in defining the structure and dynamics of aqueous solutions has a long but somewhat checkered history. In their extensive review of ionic hydration, Hinton and Amis¹ cited 685 references (the first as early 1900) but in the end concluded that 'the field is in a state of confusion'. Even the answer to such an apparently simple question like 'what is the hydration number of Na^+ ?' remained uncertain with estimates ranging from 1 to 80!

In the late 1970's, a revolution occurred in our thinking about aqueous solutions and hydration phenomena. Instead of focusing attention on a single parameter (*the* hydration number, *the* bond length, *the* geometry of the ion-water moiety) solution scientists began to realize that what actually mattered was the *distribution* of these quantities which reflects the disordered and dynamic nature of the liquid state generally. This philosophy can put into a compact form through the concept of *partial radial distribution functions* $g_{\alpha\beta}(r)$ where $\alpha, \beta \in \text{M, X, O, H}$ for a salt M_qX_p dissolved in water, H_2O .

Consider an α -type particle at the origin and ask what is the average number of β -type particles that occupy a spherical shell of radius r and thickness dr at an instant of time. That number is given by

$$dn_{\alpha}^{\beta} = 4\pi\rho_{\beta}g_{\alpha\beta}(r)r^2dr \quad (1)$$

Here $\rho_{\beta} = N_{\beta}/V$, and N_{β} is the number of β -species contained in the sample of volume V . Two 'typical' forms for $g_{\alpha\beta}(r)$ are shown in Figure 1a referring to a strongly coordinated liquid ('slow exchange') and 1b illustrating a weakly coordinated liquid ('fast exchange').

It follows from the definition of $g_{\alpha\beta}(r)$ in equation 1 that the value of the integral

$$4\pi\rho_{\beta}\int_0^{r_s} g_{\alpha\beta}(r)r^2dr \quad (2)$$

Professor John Enderby F.R.S. is the H.O. Wills Professor of Physics in the University of Bristol. He was educated at Westminster College and the University of London. He was seconded to the Institut Laue Langevin in Grenoble, France between 1985–1988 as the British Director and has, in addition, held Senior visiting positions at the Battelle Research Institute (Columbus, Ohio), the Argonne National Laboratory (Illinois), and the Universities of Quelph (Canada) and Leiden (Netherlands). He was elected a Fellow of the Royal Society in 1985 and has served on its Council. He is an elected member of Academia Europaea, a Fellow of the Institute of Physics (at present on Council), and a member of the Particle Physics and Astronomy Research Council. He works on the structural and electronic properties of liquids and was awarded the Guthrie Medal of the Institute of Physics in 1994.

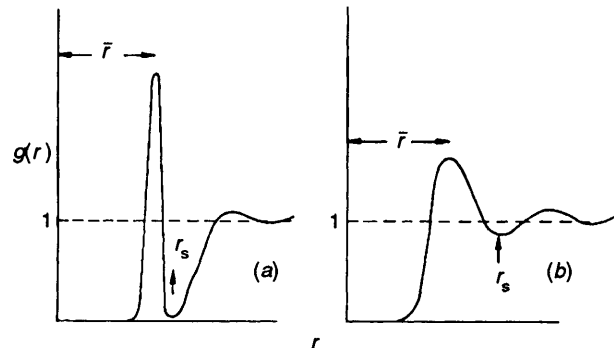


Figure 1 Generic radial distribution functions for (a) a well-coordinated liquid with a long-lived coordination shell, and (b) a weakly coordinated liquid.

is the running coordination number, *i.e.*, the average number of β atoms within a sphere of radius r_s for an α atom chosen to be at the origin. If we specify this to the distribution of oxygen atoms in water around the cation M^{p+}) and r_s is chosen to correspond to the first minimum in $g_{\text{MO}}(r)$, the value of the running coordination number is usually referred to as the coordination number \bar{n}_{M} . We can, if we so wish, define the 'hydration' number, n , as this coordination number but we must recognize that the interaction between ions and water is long-ranged and what is counted as 'bound' water is arbitrary. The *fundamental* quantity is $g_{\text{MO}}(r)$, and since different experiments probe different ranges of $g_{\text{MO}}(r)$, it is no surprise that 'hydration numbers' reported by various workers differ by large factors. There is, of course, less ambiguity for well-hydrated ions such as Ni^{2+} where the ion-water binding time, τ_m , is $\sim 10^{-5}\text{s}$ for in this case $g_{\text{NiO}}(r)$ will resemble Figure 1a. But for many ions, τ_m is $\sim 10^{-11}\text{s}$ so that the classical concept of 'hydration' needs refinement and deeper analysis.

Further insight can be gained if we know $g_{\text{MH}}(r)$ for this is an additional check on the coordination number and the stability of the first hydration shell, and allows the distribution of local geometries to be better described.

2 Neutron Diffraction and the Determination of $g_{\text{MO}}(r)$ and $g_{\text{MH}}(r)$

If neutrons are incident on a liquid containing several nuclear species the intensity of the scattered neutrons, $I(k)$ is given by

$$I(k) = \sum_{\alpha} \sum_{\beta} b_{\alpha} b_{\beta} \left\langle \sum_{i(\alpha)i(\beta)} \exp[i\mathbf{k}(\mathbf{r}_i(\beta) - \mathbf{r}_i(\alpha))] \right\rangle \\ = N \left[\sum_{\alpha} c_{\alpha} b_{\alpha}^2 + \sum_{\beta} c_{\alpha} c_{\beta} b_{\alpha} b_{\beta} [S_{\alpha\beta}(k) - 1] \right] \quad (3)$$

with $c_{\alpha} = N_{\alpha}/N$. In equation 3 $\mathbf{r}_i(\alpha)$ denotes the position of the i^{th} nucleus of α -type characterized by a neutron scattering length b_{α} and \mathbf{k} is the scattering vector whose modulus, k , for elastic scattering (*i.e.* $|\mathbf{k}_0| = |\mathbf{k}_1|$), is given by

$$k = 4\pi \sin \theta / \lambda_0 \quad (4)$$

where θ is half the scattering angle and λ_0 is the wavelength of the incident neutrons. The angular brackets show that an ensemble average has been taken, and $S_{\alpha\beta}(k)$ are the *partial structure*

factors Each $S_{\alpha\beta}(k)$ can be inverted to yield $g_{\alpha\beta}(r)$ through the Fourier transformation

$$g_{\alpha\beta}(r) = 1 + \frac{V}{2\pi^2 N r} \int dk (S_{\alpha\beta}(k) - 1) k \sin kr$$

Thus $S_{MO}(k)$ and $S_{MH}(k)$ can in principle yield the real space distribution functions $g_{MO}(r)$ and $g_{MH}(r)$ which are necessary if a proper description of ionic hydration is to be given. Unfortunately the contribution of these partial structure factors to the scattered intensity is very small, even for relatively concentrated solutions (Figure 2a)

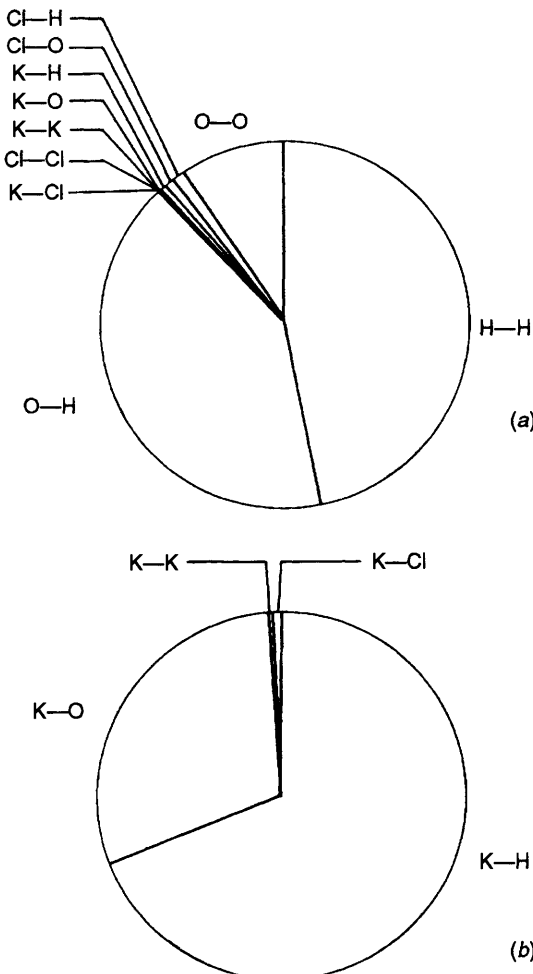


Figure 2 The relative weighting of the various contributions to a neutron diffraction experiment (a) total scattering function for a 1 molal solution of KCl in water, (b) the first order difference function for the same solution with $^{39}\text{K} \rightarrow ^{41}\text{K}$

Suppose, however, that $I(k)$ is determined for two aqueous solutions equivalent in all respects except that the isotopic state of the cation is changed. Since neutron scattering is a nuclear process, the scattering length of the cation will in general be different for the two solutions. We denote the changed species by α and the associated scattering lengths by b_α and b'_α . The two $I(k)$'s will not be identical, and the difference between them $\Delta_a(k)$ will contain only those structure factors associated with the cation, those due to the water having been 'differenced out'. Likewise the Fourier transform of $\Delta_a(k)$, $\Delta G_a(r)$, will not contain any terms due to the bulk water and will have the form

$$\Delta G_a(r) = c_a \Delta b_a \sum_{\beta \neq a} 2c_\beta b_\beta [g_{\alpha\beta}(r) - 1] + c_a^2 \Delta b_a^2 [g_{aa}(r) - 1] \quad (5)$$

where $\Delta b_a = b_a - b'_a$ and $\Delta b_a^2 = b_a^2 - b'^2_a$

As it stands, equation 5 is not very transparent, but an example will make its significance clear. Consider a 1 molal KCl/ D_2O^+ aqueous solution and suppose that the isotopic state of the potassium has been changed from ^{39}K to ^{41}K . This produces a change in the scattering length of the potassium, Δb_K , of 1.21 fm (Table 1). Formally, $\Delta G_K(r)$ consists of four terms given by equation 6

$$\begin{aligned} \Delta G_K(r) = & 2c_K c_O (\Delta b_K) b_O [g_{KO}(r) - 1] \\ & + 2c_K c_D (\Delta b_K) b_D [g_{KD}(r) - 1] \\ & + 2c_K c_C (\Delta b_K) b_C [g_{KC}(r) - 1] \\ & + c_K^2 \Delta b_K^2 [g_{KK}(r) - 1] \end{aligned} \quad (6)$$

but in practice only the first two matter (Figure 2b). Thus, the method has eliminated the water terms and the difference function $\Delta G_K(r)$ reflects almost totally the two radial distribution function $g_{KO}(r)$ and $g_{KD}(r)$. This approach solution was first proposed by Soper *et al.*² and has since been applied to a wide variety of aqueous solutions and is today known as the 'first difference' method.

In the last few years, it has become possible to take the method a stage further and separate out $g_{MO}(r)$ and $g_{MD}(r)$ from $\Delta G_M(r)$. Essentially $\Delta G_M(r)$ is measured for both heavy water solutions ($b_D = 6.67$ fm) and light water solutions ($b_H = -3.74$ fm). In an obvious notation and for the KCl/ D_2O example above

$$\Delta G_K^D(r) \cong 2c_K c_O (\Delta b_K) b_O [g_{KO}(r) - 1] + 2c_K c_D (\Delta b_K) b_D [g_{KD}(r) - 1]$$

and

$$\Delta G_K^H(r) \cong 2c_K c_O (\Delta b_K) b_O [g_{KO}(r) - 1] + 2c_K c_H (\Delta b_K) b_H [g_{KH}(r) - 1]$$

so that

$$g_{KH} = 1 + \frac{\Delta G_K^D(r)}{2c_K c_D (\Delta b_K) b_D} - \frac{\Delta G_K^H(r)}{2c_K c_H (\Delta b_K) b_H}$$

and

$$g_{KO}(r) = 1 + \frac{b_H \Delta G_K^D(r) - b_D \Delta G_K^H(r)}{2c_K c_O (\Delta b_K) b_O [b_H - b_D]} \quad (8)$$

provided H and D can be treated as isomeric [*i.e.* $g_{KD}(r) = g_{KH}(r)$]

These equations represent 'second order differences' and as such demand careful and precise experimentation. Nevertheless, the method has been successfully applied to Ni^{2+} and Cr^{3+} and doubtless further cations will be studied at this level of detail in the future.

In summary neutron diffraction with isotopic substitution allows, at the first difference level a linear combination, of $g_{MO}(r)$ and $g_{MH}(r)$, denoted $\Delta G_M(r)$, to be determined. This combination can be decomposed into the individual radial distribution function $g_{MO}(r)$ and $g_{MH}(r)$, if second order differences, involving $\text{H} \rightarrow \text{D}$ substitutions, are taken. In an analogous way, the hydration of anions can be studied by isotopic substitution, the derived quantities being $\Delta G_X(r)$, $g_{XH}(r)$, and $g_{XO}(r)$. Detailed information is available for the chloride anion and will be discussed at the end of this article.

3 The Scope of Difference Method

The only requirement for the application of the method is the existence of two or more stable (or very long lived) isotopes of the same element with a neutron scattering length difference $\Delta b \geq 1$ fm (1 fm = 10^{-15} m). A list of isotopes and the relevant scattering length data given in Table 1 demonstrate that a wide variety of ions of direct interest to solution science can be studied.

* D_2O is the preferred solvent for neutron diffraction but recently experiments have been successfully carried out in H_2O .³

Table 1 Naturally occurring nuclides (with isotopes) of relevance to solution studies

Element	Mass No A	Average Isotopic Abundance (%)	b (fm)	Δb _{max} (fm)	Element	Mass No A	Average Isotopic Abundance (%)	b (fm)	Δb _{max} (fm)
H	1	99.985	— 3.74	10.41	Ag	107	51.839	7.64	3.45
	2	0.015	6.67			109	48.161	4.19	—
	6	7.59	2.00			106	1.25	—	—
Li	7	92.5	— 2.22	4.22	Cd	108	0.89	—	—
	14	99.634	9.37			110	12.49	—	—
						111	12.80	—	15.4
N	15	0.366	6.44	2.93	In	112	24.13	7.4	—
	24	78.99	5.5			113	12.22	— 8.0	—
	25	10.00	3.6			114	28.73	6.4	—
Mg	26	11.01	4.9	1.9	Te	116	7.49	7.1	—
	32	95.02	2.80			117	4.3	5.39	1.39
	33	0.75	4.74			118	95.7	4.00	—
S	34	4.21	3.48	1.94	Te	120	0.096	—	—
	36	0.02	—			122	2.60	3.8	—
	35	75.77	11.66			123	0.908	— 0.05	—
Cl	37	24.33	3.08	8.58	Te	124	4.716	7.95	8.0
	39	93.248	3.79			125	7.14	5.01	—
	40	0.0117	—			126	18.95	5.55	—
K	41	6.730	2.58	1.21	Ba	128	31.96	5.88	—
	40	96.941	4.99			130	33.80	6.01	—
	42	0.647	3.15			130	0.106	— 3.6	—
Ca	43	0.135	0.2	4.79	Ba	132	0.101	7.8	—
	44	2.086	1.80			134	2.417	5.7	—
	46	0.004	2.55			135	6.592	4.66	2.16
Ca	48	0.187	1.5	1.21	Ce	136	7.852	4.90	—
	46	8.0	4.73			137	11.23	6.82	—
	47	7.3	3.49			138	71.70	4.83	—
Tl	48	73.8	— 5.94	11.87	Ce	138	0.19	5.80	—
	49	5.5	1.00			140	0.25	6.70	1.95
	50	5.4	5.93			142	88.48	4.84	—
V	50	4.345	7.60	8.00	Nd	142	11.08	4.75	—
	51	83.789	— 0.4			143	27.13	7.7	—
	50	4.345	— 4.50			144	12.18	—	6.3
Cr	52	83.789	4.91	9.11	Nd	144	23.80	2.4	—
	53	9.501	— 4.20			145	8.30	—	—
	54	2.365	4.55			146	17.19	8.7	—
Fe	54	5.8	4.2	13.7	Sm	148	5.76	5.7	—
	56	91.72	10.03			150	5.64	5.28	—
	57	2.2	2.3			150	3.1	— 3	—
Ni	58	0.28	15.0	13.7	Sm	152	15.0	14.3	—
	58	68.27	14.4			154	11.3	7.19	—
	60	26.10	2.8			154	13.8	— 24	19.3
Ni	61	1.13	7.60	23.10	Eu	156	7.4	14.3	—
	62	3.59	— 8.70			157	26.7	— 5.00	—
	64	0.91	— 0.38			158	22.7	9.7	—
Cu	63	69.17	6.43	4.2	Gd	158	47.8	5.00	3.22
	65	30.83	10.6			159	52.2	8.22	—
	64	48.6	5.23			160	0.20	—	—
Zn	66	27.9	5.98	2.35	Eu	160	2.18	—	—
	67	4.1	7.58			161	14.80	13.0	—
	68	18.8	6.04			162	20.47	6.3	7.7
Ga	70	0.6	—	1.48	Gd	163	15.65	11.3	—
	69	60.1	7.88			164	24.84	8.9	—
	71	39.9	6.40			165	21.86	9.15	—
Sr	84	0.56	—	1.48	Dy	166	0.06	—	—
	86	9.86	5.68			167	0.10	—	42.9
	87	7.00	7.41			168	2.34	— 0.7	—
Zr	88	82.58	7.16	3.3	Dy	169	18.9	—	—
	90	51.45	6.5			170	25.5	—	—
	91	11.22	8.8			171	33.6	10.4	7.4
Zr	92	17.15	7.5		Er	172	33.95	3.0	—
	94	17.38	8.3			173	26.8	8.7	—
	96	2.80	5.5			174	14.9	9.3	—
Pd	102	1.020	—	2.3	Er	175	0.13	—	—
	104	11.14	5.5			176	3.05	6.8	—
	105	22.33	6.4			177	14.3	9.7	—
Pd	106	27.33	4.1	2.3	Yb	178	21.9	9.61	16.3
	108	26.46	—			179	16.12	9.56	—
	110	11.72	—			180	31.8	23.05	—

Table 1 (cont.)

Element	Mass No. A	Average Isotopic Abundance (%)	b (fm)	$ \Delta b _{\max}$ (fm)
Hf	176	12.7	8.7	
	174	0.162	10.91	
	176	5.206	6.61	
	177	18.606	0.71	12.5
	178	27.297	5.9	
	179	13.629	7.46	
	180	35.100	13.2	
W	180	0.13	—	
	182	26.3	7.04	
	183	14.3	6.59	8.28
	184	30.67	7.55	
	186	28.6	— 0.73	
	184	0.02	—	
	186	1.58	12.0	
Os	187	1.6	9.7	
	188	13.3	7.8	4.2
	189	16.1	11.0	
	190	26.4	11.4	
	192	41.0	11.9	
	190	0.01	9	
	192	0.79	9.9	
Pt	194	32.9	10.55	2.72
	195	33.8	8.91	
	196	25.3	9.89	
	198	7.2	7.83	
	196	0.14	30.3	
	198	10.02	—	
	199	16.84	16.9	
Hg	200	23.13	—	13.4
	201	13.22	—	
	202	29.80	—	
	204	6.85	—	
Tl	203	29.524	6.9	2.6
	205	70.476	9.5	

Notes

(i) This list, though substantially based on the Sears (reference *a*) compilation, differs for those isotopes where new information is now available. Several isotopes have been measured or re-measured by Koester and co-workers and the results are reported in issues of the *Zeitschrift für Physik A* (1980–1990). For isotopes where resonance effects are important around thermal energies, (notably Cd, In, and the lanthanides), the values quoted refer to a specific wavelength *e.g.* b for ^{164}Dy is for $\lambda = 0.499 \text{ \AA}$. A full description of how to convert to other wavelengths is given in Cossy *et al.* (reference *b*) and the 'raw' data provided by Sears needs to be carefully interpreted. $|\Delta b|_{\max}$ is calculated for isotope pairs *excluding* those for which the abundance is less than 0.1%.

(ii) To calculate b for the naturally occurring element, sum the products of isotopic abundance and isotopic scattering length and divide by 100, *e.g.* $b(^{\text{nat}}\text{Ni}) = [68.27 \times 14.4 + 26.10 \times 2.8 + 1.13 \times 7.6 + 3.59 \times (-8.70) + 0.91 \times (-0.38)]/100 = 10.3 \text{ fm}$

References

(a) V. F. Sears, AECL Report 8490, Chalk River Nuclear Laboratories Canada (1984)

(b) C. Cossy, A. C. Barnes, J. E. Enderby, and A. E. Merbach, *J. Chem. Phys.*, 1989, **90**, 3254

3.1 Some Specific Examples**3.1.1 Ni^{2+}**

The first example is Ni^{2+} which is particularly favourable for the difference method. A convenient substitution is $^{\text{nat}}\text{Ni} \rightarrow ^{62}\text{Ni}$ which yields $\Delta b = 18.9 \text{ fm}$. An example of $\Delta G_{\text{Ni}}(r)$ is shown in Figure 3 and the relevant structural parameters for a variety of concentrations and counter ions are listed in Table 2. The form of $\Delta G_{\text{Ni}}(r)$ and the stability of the first hydration shell against changes in concentration, temperature, and counter ion 'decisively support the accepted stoichiometry for the complex (*i.e.* $\text{Ni}(\text{OH}_2)_6$)' (Hunt and Friedman in reference 4).

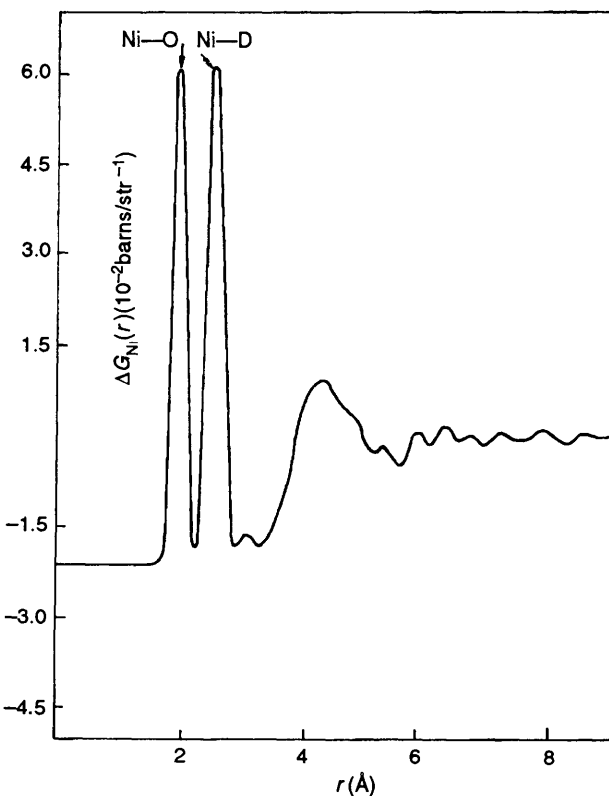


Figure 3 The first-order difference function $\Delta G_{\text{Ni}}(r)$ for a 1.46 molal solution of NiCl_2 in D_2O (1 barn = 10^{-28} m^2). In this and later figures, the unphysical structure below the first peak has, for clarity, been suppressed.

Table 2 Hydration properties of Ni^{2+} in D_2O

Electrolyte	Molality	\bar{n}_{Ni}^0	$\bar{r}_{\text{NiO}}/\text{\AA}$	$\sigma_{\text{NiO}}/\text{\AA}$	\bar{n}_{D}	$\bar{r}_{\text{NiD}}/\text{\AA}$	$\sigma_{\text{NiD}}/\text{\AA}$
NiCl_2	4.41	5.8(2)	2.07(2)	0.27(3)	—	2.67(2)	0.38(3)
	3.05	5.8(2)	2.07(2)	0.27(3)	—	2.67(2)	0.38(3)
	2.0	5.9(1)	2.06(2)	0.30(3)	11.7(2)	2.67(2)	0.36(3)
	1.46	5.8(3)	2.07(2)	—	11.6(3)	2.67(2)	0.34(3)
	0.50	5.9(2)	2.07(2)	0.30(3)	11.4(4)	2.68(2)	0.36(3)
	3.80	5.8(2)	2.07(2)	0.26(3)	—	2.67(2)	0.36(3)

In this and subsequent tables σ_{MO} and σ_{MD} are the full-width at half-maximum of the principal peaks in $\Delta G_{\text{M}}(r)$

The *instantaneous* geometry of a nickel complex shown in Figure 4 and is essentially constant for solutions in the concentration range 0.1 to 4 molal. The *mean value* of the so-called 'tilt angle' ϕ obtained from

$$\cos\phi = \frac{\bar{r}_{\text{NiH}}^2 - (\bar{r}_{\text{OH}}^2 + \bar{r}_{\text{NiO}}^2)}{2\bar{r}_{\text{NiO}}\bar{r}_{\text{OH}}\cos(\theta/2)}$$

where θ is the water bond angle, though frequently quoted in the past is, in fact, misleading^{5,6}. This is because the water molecules in the hydration shell undergo significant 'wagging' motions and, as explained earlier, a more fundamental quantity is the *probability density*, $P(\cos\phi)$. With the aid of a simple model Powell and Neilson⁶ were able to show that $P(\cos\phi)$ is a broad function, with a weak tendency to peak near, but not at, $\phi = 0$.

Since H and D have scattering lengths of different sign, it is possible to isolate $g_{\text{NiO}}(r)$ from $\Delta G_{\text{Ni}}(r)$ by choosing a 'null' mixture of H_2O and D_2O as the solvent. There are small corrections due to the presence of $g_{\text{NiNi}}(r)$ and $g_{\text{NiCl}}(r)$ in $\Delta G_{\text{Ni}}(r)$ but these can be safely neglected. This experiment was performed by Powell *et al.*³ for a 2 molal solution of NiCl_2 with the

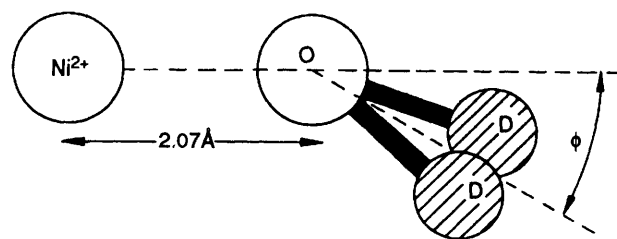


Figure 4 The instantaneous geometry of the nickel–water complex. ϕ is the so-called ‘tilt angle’ and is a function of time.

results shown in Figure 5. At the same time the second difference method as exemplified by equation 7 yields $g_{\text{NiH}}(r)$ exactly (Figure 6). These two functions allow several new conclusions to be drawn. They confirm (if confirmation were needed) that the first peak in $\Delta G_{\text{Ni}}(r)$ is indeed due to $g_{\text{NiO}}(r)$ and that the stoichiometry of the complex is $\text{Ni}(\text{OH}_2)_6$. More significant is the fact that peaks in $g_{\text{NiO}}(r)$ and $g_{\text{NiH}}(r)$ are separated for both the first coordination shell [which is clear from the form of $\Delta G_{\text{Ni}}(r)$] and for the second coordination shell [a result not evident from $\Delta G_{\text{Ni}}(r)$]. Thus, the *orientational* order of the water molecules driven by divalent ions persists over length scales of 6 Å or more. This experimental result was, in fact, anticipated by Dietz, Reide, and Heinzinger⁷ in their pioneering computer simulation studies of Mg^{2+} in solution.

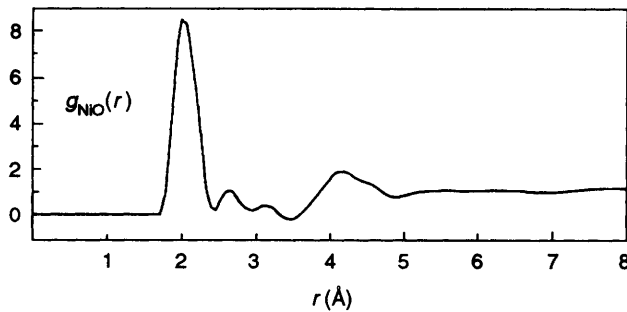


Figure 5 The radial distribution function $g_{\text{NiO}}(r)$ (Reference 3).

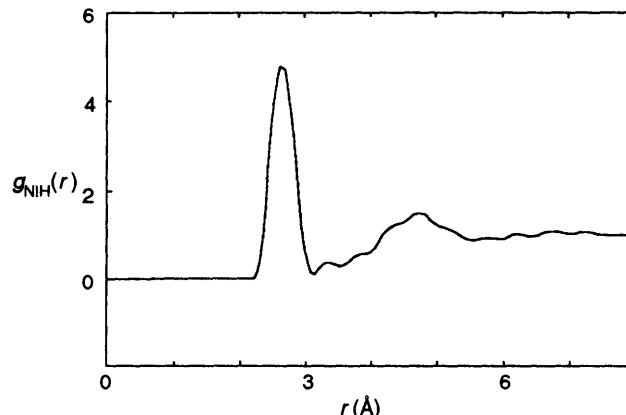


Figure 6 The radial distribution function $g_{\text{NiH}}(r)$ (Reference 3).

3.1.2 Cr^{3+}

It is, of course, well established that the chromium(III) ion in aqueous solutions coordinates six water molecules in the first hydration sphere. Experiments based on isotopic dilution show that the residence time of the oxygen atoms in the first hydration shell is long (approximately 1×10^6 s). The lifetime of the first-shell water hydrogen atoms is much shorter ($\sim 10^{-5}$ s) but

nevertheless the Cr^{3+} – H_2O moiety is clearly very stable. It is therefore of interest to compare $\Delta G_{\text{Cr}}(r)$, $g_{\text{CrO}}(r)$, and $g_{\text{CrH}}(r)$ with the equivalent quantities for other cations in solution.

Broadbent, Neilson, and Sandström⁸ exploited the substitution ${}^{\text{nat}}\text{Cr} \rightarrow {}^{53}\text{Cr}$ which gives a Δb value of 7.56 fm. To avoid the anion displacing water as a ligand, Broadbent *et al.* worked with a perchlorate solution at 2.2 molal. They also used $\text{H} \rightarrow \text{D}$ substitutions in order to obtain a second difference and their results for $\Delta G_{\text{Cr}}(r)$, $g_{\text{CrO}}(r)$, and $g_{\text{CrH}}(r)$ are shown in Figures 7, 8, and 9 and in Table 3. The comparison with the corresponding data for Ni^{2+} is instructive; the structure of the first coordination shell and the persistence of orientational order into the second shell and beyond confirm the strongly hydrating character of Cr^{3+} .

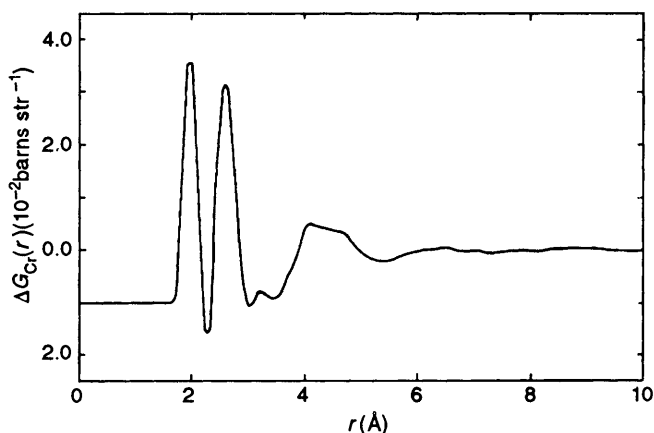


Figure 7 The first-order difference function $\Delta G_{\text{Cr}}(r)$ for Cr^{3+} in D_2O (Reference 8).

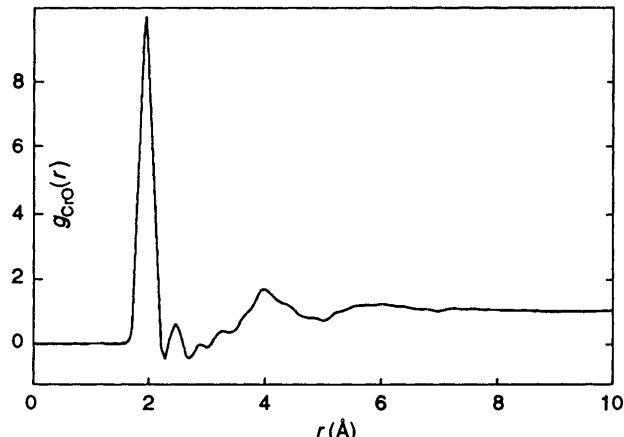


Figure 8 The radial distribution function $g_{\text{CrO}}(r)$ (Reference 8).

3.1.3 Fe^{2+} and Fe^{3+}

In view of the general interest in electron-transfer reactions and, specifically, the ferrous \rightarrow ferric exchange mechanism, a comparison of the hydration properties of Fe^{2+} and Fe^{3+} is of considerable relevance. Such a study was undertaken by Herdman and Neilson⁹ with the results shown in Figure 10 and Table 4. They clearly confirm the existence of well-defined octahedral complexes with r_{FeO} shifted by 0.1 Å for $\text{Fe}^{2+} \rightarrow \text{Fe}^{3+}$. This observation is in excellent agreement with the MD study of Kumar and Tembe¹⁰ although the absolute ion–oxygen separation predicted by theory differs from experiment by about 0.15 Å. At the $\Delta G_{\text{Fe}}(r)$ level, it is clear that orientational effects in the second shell are more pronounced for ferric ions, although to make this statement fully quantitative second-order difference with $\text{H} \rightarrow \text{D}$ substitutions are necessary.

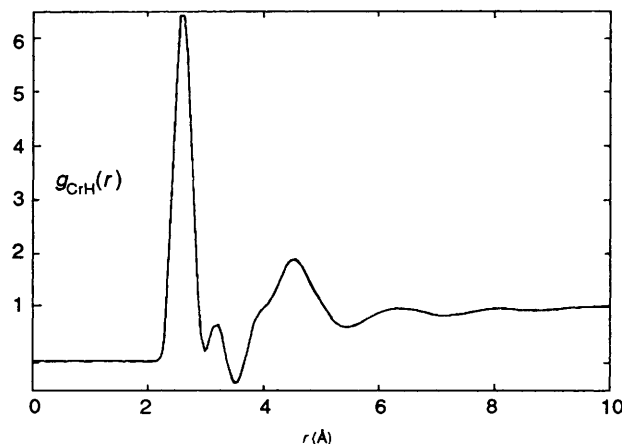


Figure 9 The radial distribution function $g_{\text{CrH}}(r)$ (Reference 8).

Table 3 Hydration properties of Cr^{3+}

Electrolyte	Molality	\bar{n}_{M}	$\bar{r}_{\text{MO}}/\text{\AA}$	$\sigma_{\text{MO}}/\text{\AA}$	$\bar{n}_{\text{M}}^{\text{H}}$	$\bar{r}_{\text{MH}}/\text{\AA}$	$\sigma_{\text{MH}}/\text{\AA}$
$\text{Cr}(\text{ClO}_4)_3$	2	6.0(5)	1.98(2)	0.27(4)	11.5(5)	2.60(3)	0.36(4)

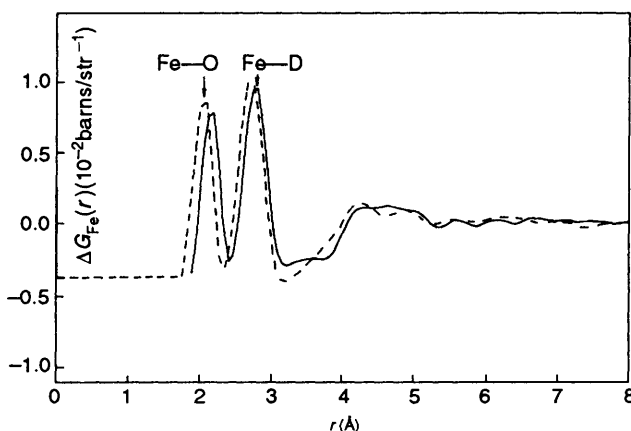


Figure 10 The first-order difference function $\Delta G_{\text{Fe}}(r)$ for (a) Fe^{2+} (full line), and (b) Fe^{3+} (broken line). Taken from Reference 9.

Table 4 Hydration properties of Fe^{2+} in 1 molal iron chloride in heavy water and Fe^{3+} in 1.5 molal iron nitrate in heavy water

Cation	$\bar{n}_{\text{Fe}}^{\text{O}}$	$\bar{r}_{\text{FeO}}/\text{\AA}$	$\sigma_{\text{FeO}}/\text{\AA}$	$\bar{n}_{\text{Fe}}^{\text{D}}$	$\bar{r}_{\text{FeD}}/\text{\AA}$	$\sigma_{\text{FeD}}/\text{\AA}$
Fe^{2+}	6.0(3)	2.13(2)	0.28(2)	12.1(5)	2.75(5)	0.36(3)
Fe^{3+}	6.0(2)	2.01(2)	0.32(2)	12.0(5)	2.68(3)	0.40(3)

3.1.4 The lanthanides

‘Despite the large number of attempts made in the last twenty years to determine the coordination number and structure of the tripotitive lanthanide ions in aqueous solution, it is as yet still unclear whether a coordination number change from nine to eight occurs along the series or not. This uncertainty hinders the mechanistic description of the dynamic processes which are taking place on these solvates.’ (Helm and Merbach, in reference 11.)

As can be seen from Table 1, the lanthanides are well suited to the difference method and a programme of research, initiated by

Cossy *et al.*¹² is underway in the Lausanne group led by Professor Merbach. A summary of the results obtained so far is given in Table 5 and the form of $\Delta G_{\text{Ln}}(r)$ clearly resembles that obtained for ferric iron as the example in Figure 11 shows. The data confirm that there is indeed a decrease in coordination number from nine to eight along the lanthanide series. The intermediate value of 8.5 found for Sm^{3+} indicates the presence of an equilibrium distribution of eight and nine coordinated aqua ions. Helm and Merbach¹¹ have analysed the full width at half height of the first two peaks in $\Delta G_{\text{Ln}}(r)$ and have concluded in the light of this and other spectroscopic evidence that for the lighter elements, \bar{r}_{LnO} is in fact bimodal.

Table 5 A comparison of the coordination numbers (CN), the Ln^{3+} -oxygen (\bar{r}_{MO}) distances, the Ln^{3+} -deuterium (\bar{r}_{MD}) distances, and the corresponding full width at half height (σ) obtained from neutron diffraction studies on aqueous $\text{Ln}(\text{ClO}_4)_3$ solutions

Ln^{3+}	Molality	$\bar{n}_{\text{Ln}}^{\text{O}}$	$\bar{r}_{\text{MO}}/\text{\AA}$	$\bar{r}_{\text{MD}}/\text{\AA}$	$\sigma_{\text{MO}}/\text{\AA}$	$\sigma_{\text{MD}}/\text{\AA}$
Nd	1.8 m	8.9(2)	2.50(2)	3.14(3)	0.30(2)	0.42(3)
Nd	0.3 m	8.8(2)	2.52(2)	3.15(3)	0.28(2)	0.41(3)
Sm	1.0 m	8.5(2)	2.46(2)	3.11(3)	0.31(2)	0.43(3)
Dy	1.0 m	7.9(2)	2.38(2)	3.03(3)	0.26(2)	0.36(3)
Dy	0.3 m	7.9(2)	2.39(2)	3.03(3)	0.25(2)	0.35(3)
Yb	1.0 m	7.9(2)	2.32(2)	2.98(3)	0.24(2)	0.33(3)

Taken from L. Helm and A. E. Merbach, *Eur. J. Solid State Inorg. Chem.*, 1991, 28, 245.

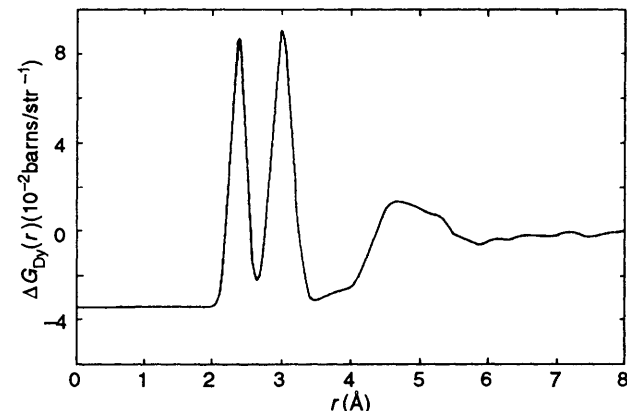


Figure 11 The first-order difference function $\Delta G_{\text{Dy}}(r)$ for Dy^{3+} in D_2O (Reference 12).

3.1.5 Li^+ , Ag^+ (approximately isomorphic with Na^+) and K^+

The first-order difference method of neutron diffraction can be applied directly to Li^+ and K^+ . The sodium ion can be investigated at an approximate level by total X-ray diffraction and by isomorphic substitution and using the Na^+/Ag^+ pair.¹³ A summary of experimental and theoretical data is given in Table 6.

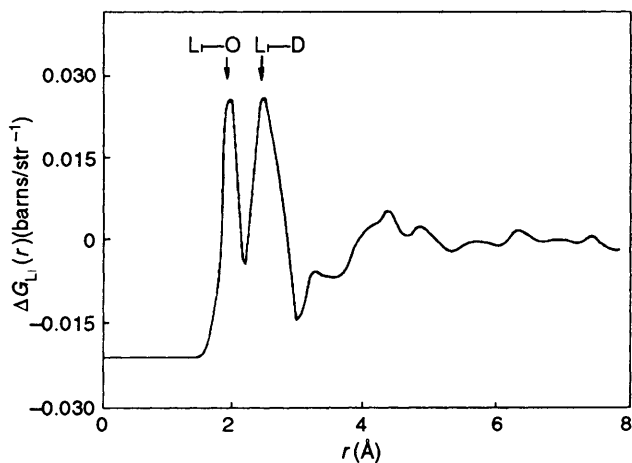
The studies have shown that Li^+ has a well-defined hydration shell (Figure 12) characterized by the two resolved peaks in $\Delta G_{\text{Li}}(r)$. The value of \bar{n}_{LiO} changes with concentration, approaching 6 in the dilute limit and dropping well below 4 at high concentrations. Computer simulations give a value of 6 for Li^+ at infinite dilution, with structural parameters in broad agreement with experiment. It should, however, be pointed out that although the two resolved peaks in $\Delta G_{\text{Li}}(r)$ shows that this ion is well hydrated, the fact that \bar{n}_{LiO} is strongly concentration dependent and that water ion binding time is only ~ 20 ps implies that the hydration is considerably less well defined than that of divalent cations like Ni^{2+} .

Table 6 Hydration properties of Li^+ , Na^+ , Ag^+ , and K^+ in D_2O

Ion	Method	Reference	\bar{r}_{LO} (\AA)	\bar{r}_{IH} (\AA)	Coordination number \bar{n}_{MO}
Li^+	expt	1	1.95(2)	2.55(2)	5.5(3)
	MD	2	2.04	2.60	6.0
	MD	3	1.98	2.57	5.3
Na^+	expt	4	2.42(2)	—	5(1)
	MD	2	2.35	2.91	6.2
	MD	3	2.29	2.95	6.0
	MD	5	2.55	3.05	5.4
K^+	expt	6	2.71(1)	3.12(2)	5.5(5)
	MD	2	2.86	3.32	7.6
	MD	3	2.76	3.35	7.5
Ag^+	expt	7	2.41(2)	2.97(4)	4.1(3)

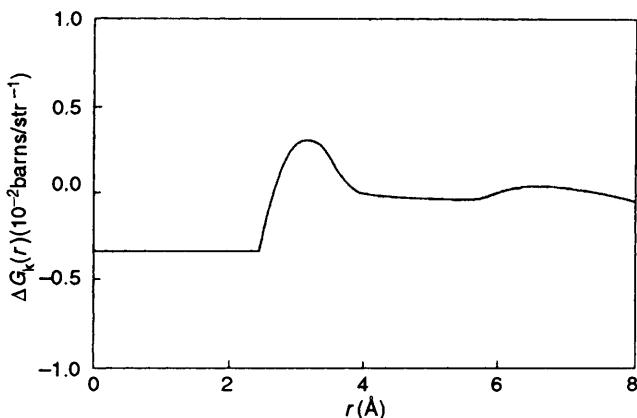
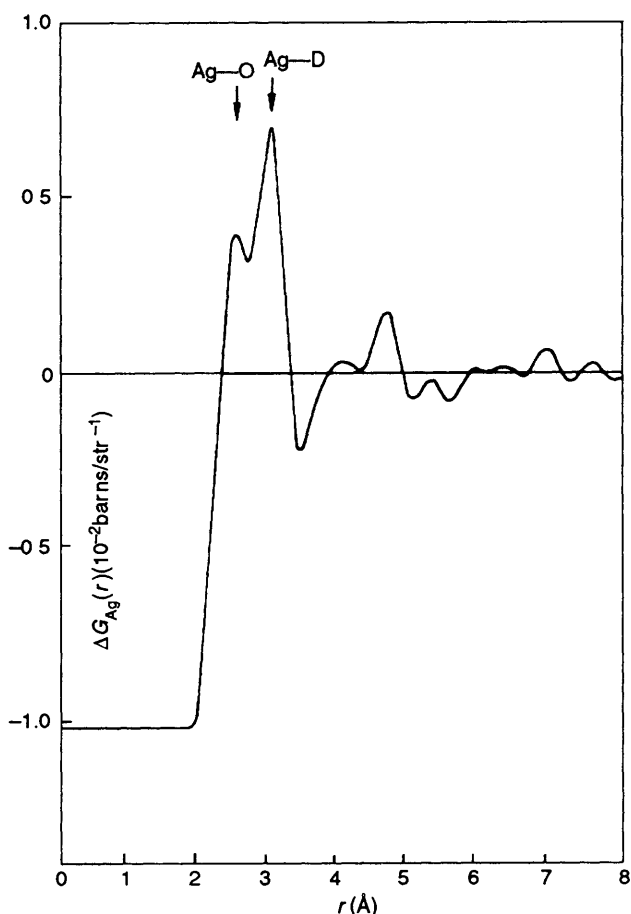
References

- 1 J. R. Newsome, G. W. Neilson, and J. E. Enderby, *J. Phys. C*, 1980, **13**, L923
- 2 D. Bounds, *Mol. Phys.*, 1985, **54**, 1335
- 3 R. W. Impey, P. A. Madden, and I. R. Macdonald, *J. Phys. Chem.*, 1983, **87**, 5071
- 4 N. T. Skipper and G. W. Neilson, *J. Phys. Condens. Matter*, 1989, **1**, 4147
- 5 S. B. Zhu and G. W. Robinson, *J. Chem. Phys.*, 1992, **97**, 4336
- 6 G. W. Neilson and N. T. Skipper, *Chem. Phys. Lett.*, 1985, **114**, 35
- 7 M. Sandstrom, G. W. Neilson, G. Johansson, and T. Yamaguchi, *J. Phys. C, Solid State Phys.*, 1985, **18**, L1115

**Figure 12** The first-order difference function $\Delta G_{\text{Li}}(r)$ for Li^+ in D_2O (see Table 6)

The comparable data for K^+ are shown in Figure 13. The absence of clearly resolved peaks in $\Delta G_{\text{K}}(r)$ is clear evidence that K^+ is weakly hydrated so that no specific dynamical significance can be attributed to water molecules located in the first shell, the coordination number simply expresses the geometrical fact that there is a high probability of finding water molecules around K^+ but the hydration shell itself is highly disordered with considerable inter-penetration of $g_{\text{KO}}(r)$ and $g_{\text{KD}}(r)$.

Sodium is monosotopic and is therefore not susceptible to the first difference method. However, Ag^+ can be studied by neutron diffraction (Figure 14) and since Ag^+ and Na^+ are, to a first approximation isomeric, $\Delta G_{\text{Ag}}(r)$ can be used as a good indication of the form for $\Delta G_{\text{Na}}(r)$. Theoretical results for $g_{\text{NaO}}(r)$ and $g_{\text{NaH}}(r)$ are shown in Figure 15. Clearly Na^+ is intermediate between Li^+ and K^+ and can be regarded as a moderately hydrated ion. This is confirmed by an X-ray study of the compound $\text{NaOH} \cdot 7\text{H}_2\text{O}$ in the solid¹⁴ which shows that the sodium–water distance varies from 2.29 Å to 2.46 Å and that the Na^+ environment is a highly distorted octahedron. This local structure contrasts with that for the well-hydrated Mg^{2+} in $\text{MgCl}_2 \cdot 12\text{H}_2\text{O}$ where the cationic environment is a regular octahedron and \bar{r}_{MgO} is 2.065 Å for all six water molecules. A

**Figure 13** The first-order difference function $\Delta G_{\text{K}}(r)$ for K^+ in D_2O (see Table 6)**Figure 14** The first-order difference function $\Delta G_{\text{Ag}}(r)$ for Ag^+ in D_2O (see Table 6)

comparison of the radial distribution functions for the oxygen atoms of the water with respect to Li^+ , Na^+ , and K^+ , together with the equivalent quantity for pure water is shown in Figure 16

3.1.6 Ca^{2+} and Sr^{2+}

The coordination properties of both Ca^{2+} and Sr^{2+} have formed the basis of several investigations both of an experimental and theoretical nature. Early experiments¹⁵ on Ca^{2+} showed that $\Delta G_{\text{Ca}}(r)$ was characterized by two peaks indicating that this divalent ion is well-coordinated although the hydration number was reported to be strongly concentration dependent (Table 7).

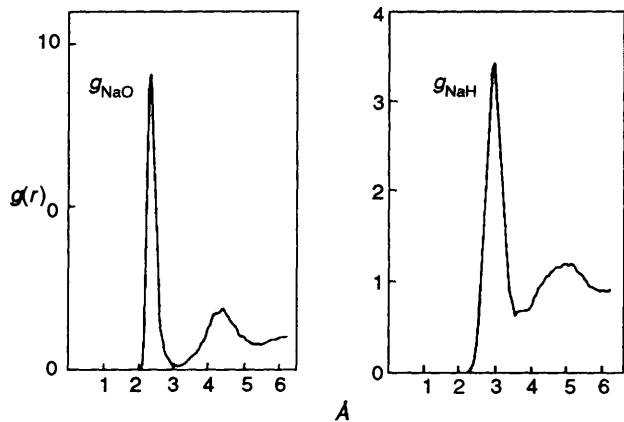


Figure 15 Theoretical radial distribution function for Na^+ in D_2O (see Table 6).

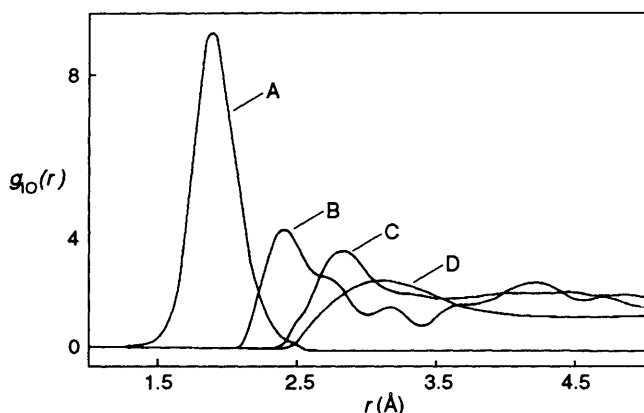


Figure 16 The radial distribution functions $g_{10}(r)$ ($\text{I} \equiv \text{Li}^+, \text{Na}^+, \text{O}^-, \text{K}^+$; A: Li^+ ; B: Na^+ ; C: O; D: K^+) (Reference 13).

Table 7 Hydration properties of Ca^{2+} in D_2O

Electrolyte	Molality	\bar{n}_{Ca}^0	$\bar{r}_{\text{CaO}}/\text{\AA}$	$\sigma_{\text{CaO}}/\text{\AA}$	$\bar{r}_{\text{CaD}}/\text{\AA}$	$\sigma_{\text{CaD}}/\text{\AA}$
CaCl_2	4.5	6.4(3)	2.41(3)	0.34(3)	3.04(3)	0.43(3)
CaCl_2	2.8	7.2(2)	2.39(2)	0.34(3)	3.02(3)	0.43(3)
CaCl_2	1.0	10.0(6)	2.46(3)	0.43(4)	3.07(3)	0.61(4)

These experiments should be repeated with the improved technology now available in order to remove some of the uncertainties. Barnes (private communication) has begun this study and reports that the hydration shell is of a more complex nature than was originally proposed by Hewish *et al.*

The other alkaline earth studied so far is Sr^{2+} .¹⁶ $\Delta G_{\text{Sr}}(r)$ was characterized by a single broad peak centred at 3.2 Å. This result implies that there is considerable penetration of $g_{\text{SrO}}(r)$ by $g_{\text{SrH}}(r)$, a consequence of a highly disordered first coordination shell.

3.1.7 Cu^{2+} and Zn^{2+}

Salmon and co-workers have studied the Jahn–Teller ion Cu^{2+} .^{17,18} Examples of $\Delta G_{\text{Cu}}(r)$ are shown in Figure 17 and are consistent with the expected E_g distortion of the six octahedrally coordinated water molecules which solvate the cupric ion. This observation raises interesting and important theoretical questions as to the meaning of the Jahn–Teller distortion in the liquid state. Accordingly, Curtiss, Halley, and Wang¹⁹ addressed this problem theoretically and have concluded that on

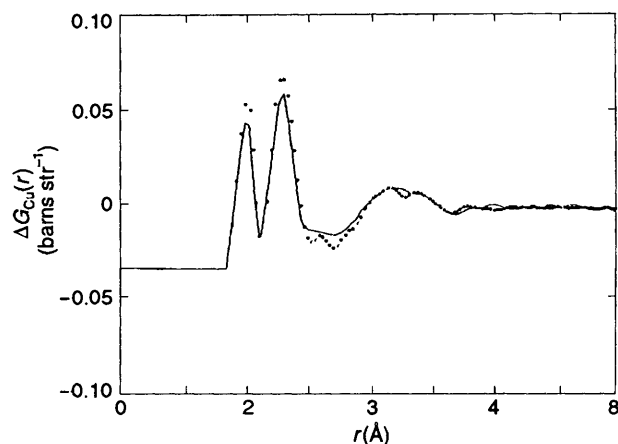


Figure 17 The first-order differences for $\Delta G_{\text{Cu}}(r)$ for (a) Cu^{2+} in D_2O with nitrate as the counter ion (full line); (b) Cu^{2+} in the D_2O with percholate as the counter ion (dotted line). The percholate data have been scaled so that the contribution to $\Delta G_{\text{Cu}}(r)$ from $g_{\text{CuO}}(r)$ is equivalent to that from the nitrate (Reference 18).

long time scales, the structure of the hydration shell must be rotationally invariant. On intermediate time scales, the shell exhibits cubic symmetry and it is only on the shortest scales where the (D_{4h}) distortion is apparent.

It has long been recognized that the strong tendency of Zn^{2+} to coordinate other ligands has made the investigation of this aquaion especially difficult. Powell *et al.*²⁰ have shown that in chloride solutions with molalities as low as 0.48, significant Zn^{2+} – Cl^- interactions occur at room temperature. In a later study Powell *et al.*²¹ investigated a 2 molal zinc solution in which the anion was methanesulfonate (triflate). The choice of the triflate ion was made in order to avoid cation–anion complexation, so that a first-order isotopic-difference study of Zn^{2+} based on the substitution ${}^{nat}\text{Zn} \rightarrow {}^{67}\text{Zn}$ should yield an unambiguous description of the hydration shell. The data for $\Delta G_{\text{Zn}}(r)$ are displayed in Figure 18 and the relevant structural parameters are listed in Table 8. It is something of a puzzle that \bar{n}_{Zn}^0 is found to be 5.3. The peak widths characteristic of $\Delta G_{\text{Zn}}(r)$ together with the spectroscopic evidence lead to the conclusion that the Zn^{2+} –water complex is relatively long-lived so that \bar{n}_{Zn}^0 might be expected to be 6 (octahedral coordination) or 4 (tetrahedral coordination). One possibility is that both species exist in solution in more or less equal proportions. Further experiments, involving changes in pH, concentration, and pressure are necessary if a complete understanding of this important ion is to be achieved.

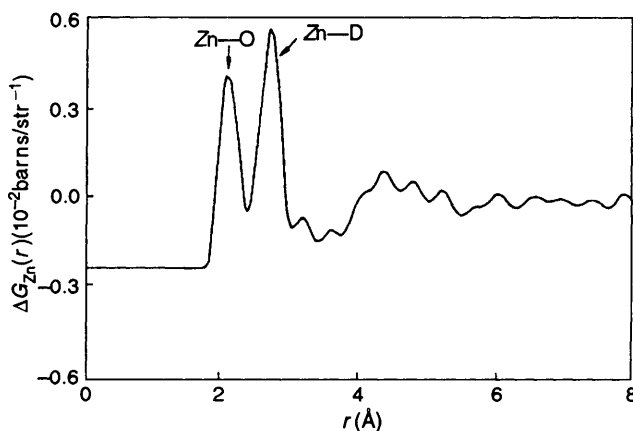


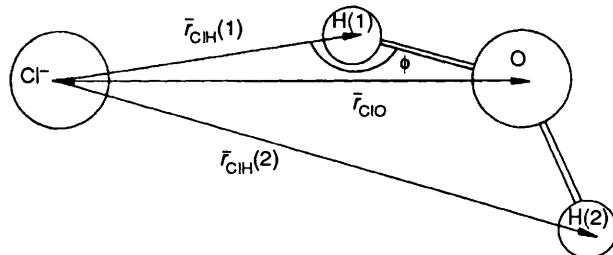
Figure 18 The first-order difference function $\Delta G_{\text{Zn}}(r)$ for Zn^{2+} in D_2O . To avoid inner sphere complexation, triflate was used as the counter ion (Reference 21).

Table 8 Hydration properties of Zn^{2+} in D_2O

Electrolyte	Molality	n_{Zn}^D	$r_{ZnD}/\text{\AA}$	$\sigma_{ZnD}/\text{\AA}$	n_{Zn}^D	$r_{ZnD}/\text{\AA}$	$\sigma_{ZnD}/\text{\AA}$
$Zn(CF_3SO_3)_2$	2.0	5.3(2)	2.09(2)	0.26(3)	10.6(2)	2.69	0.32(3)

3.1.8 Cl^-

Although several anions have been studied by the difference method, we shall focus here only on the chloride ion. This ion is a useful probe of anion properties in solution and is an important ion in its own right. In previous studies at the first difference level it was established that Cl^- has a characteristic local coordination which is remarkably insensitive to ionic concentration, counterion, and moderate changes in temperature and pressure.²² The shape of $\Delta G_{Cl}(r)$ is characterized by two well-defined peaks centred around 2.2 Å and 3.2 Å. The first of these reflects $Cl-H(1)$ interactions, whilst the second is an unresolved pair $Cl-O$ and $Cl-H(2)$. The most widely accepted geometry of the $Cl-H_2O$ interaction consistent with both experimental and theoretical studies is shown in Figure 19. For relatively low concentrations ($c < 2$ molal) the coordination number saturates at approximately 6.

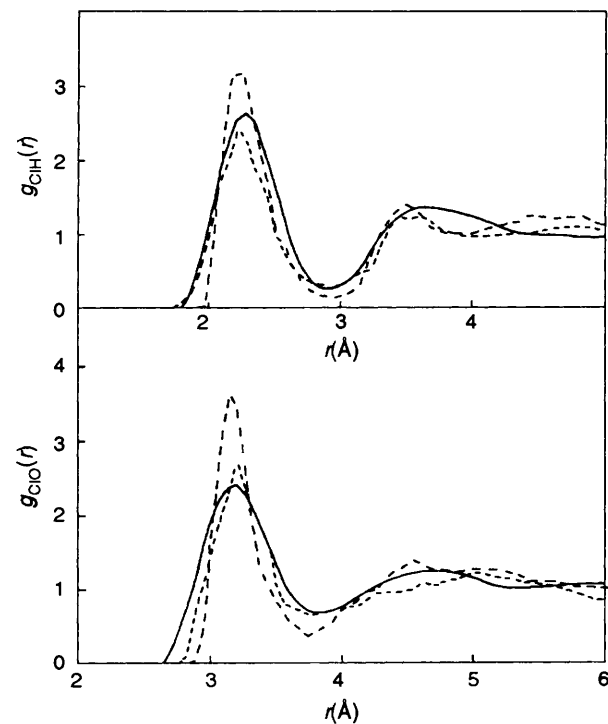
**Figure 19** The instantaneous arrangement of a water molecule near to a chloride ion

In a recent study Powell *et al.*²³ worked at the second difference level, and obtained the individual pair distribution functions $g_{ClH}(r)$ and $g_{ClO}(r)$. In this way it was possible to resolve structure in $\Delta G_{Cl}(r)$ notably around the second peak, and hence discuss the $Cl^- - H_2O$ coordination in considerable detail.

From the individual $g_{ClH}(r)$ and $g_{ClO}(r)$ and the structural parameters shown in Figure 20 and Table 9, Powell *et al.* were able to draw several firm conclusions. First, the new results decisively confirm the widely accepted geometry described in Figure 19. The 'linear' configuration is fully justified and the 'dipolar' model (which still appears in text-books from time to time) can, in agreement with all recent calculations, be finally rejected.

Secondly, the value of r_{ClH} derived directly from $g_{ClH}(r)$ of 2.28 ± 0.03 Å is in excellent agreement with previous studies based on $\Delta G_{Cl}(r)$. The first maximum in $g_{ClO}(r)$ occurs at 3.1 ± 0.1 Å. In earlier studies the position of the broad second peak in $\Delta G_{Cl}(r)$ was sometimes (incorrectly) ascribed to r_{ClO} alone with the result that the apparent chloride–oxygen distance quoted was too long by ~ 0.05 Å. This new work essentially resolved the difference noted by Magini *et al.*²⁴ between r_{ClO} distance obtained by total X-ray diffraction and by the first difference method, particularly when it is remembered that the former approach requires some degree of modelling.

The comparison of the experimental distribution functions with those derived from computer simulation is particularly instructive. Many studies of the chloride ion in solution were undertaken during the period 1976–1985. The results of these studies were, in the main, compared with experiment at the first difference [i.e. $\Delta G_{Cl}(r)$] level and, apart from a tendency to overestimate the coordination number by $\sim 30\%$, the measure of agreement secured was deemed to be satisfactory. Now we are

**Figure 20** The radial distribution functions $g_{ClH}(r)$ and $g_{ClO}(r)$ in a 2 molal $NiCl_2$ solution experiment (full line) (Reference 23), Sprik *et al.* (short-dashed line) (Reference 25), Dang *et al.* (long-dashed line) (Reference 26)**Table 9** Coordination properties of chloride in water

$r_{ClH(1)}/\text{\AA}$	$n_{Cl}^H \dagger$	$r_{ClO}/\text{\AA}$	$n_{Cl}^O \dagger$	$r_{ClH(2)}/\text{\AA}$
2.28(3)	6.4(3)	3.1(1)	7.0(4)	3.7(1)

† Because of penetration effects by water molecules outside the first coordination shell, n_{Cl}^H rather than n_{Cl}^O is the primary coordination number

in a position to make a detailed comparison at the $g_{ab}(r)$ level it is evident that even the best of the earlier simulations do not capture some essential features in the experimental data, a fact disguised by cancellation of discrepancies in the formation of the linear combination of $g_{ClH}(r)$ and $g_{ClO}(r)$ to obtain $\Delta G_{Cl}(r)$. In recent studies, Sprik *et al.*²⁵ and Dang *et al.*²⁶ have argued that many of the earlier difficulties arise from the failure to account properly for the polarizability of the water and/or the chloride ion. The results of the two recent simulations which used a polarizable water model, are in much better agreement with experiment than those from earlier studies, particularly with respect to the chloride–oxygen and chloride–hydrogen distances and coordination numbers (Figure 20). The challenge to describe satisfactorily the chloride–water coordination still remains, but the experimental partial radial distribution functions obtained by Powell *et al.*²³ indicate where improvements are required and will provide a crucial test of new and refined models.

Acknowledgements It is my great pleasure to thank my colleagues at Bristol, notably Drs George Neilson and Adrian Barnes for a long and fruitful collaboration. This brief summary does scant justice to the range of structural work undertaken by the Bristol group over the past fifteen years. I also wish to acknowledge the many helpful discussions I have had with Professor Harold Friedman at SUNY (Stony Brook). The work has been supported by the Science & Engineering Research Council and by a NATO travel grant (RG125/80).

4 References

- 1 J F Hinton and E S Amis, *Chem Rev*, 1971, **71**, 627
- 2 A K Soper, G W Neilson, J E Enderby, and R A Howe, *J Phys C Solid State Phys*, 1977, **10**, 1793
- 3 D H Powell, G W Neilson, and J E Enderby, *J Phys Condens Matter*, 1989, **1**, 8721
- 4 J P Hunt and H L Friedman, *Prog Inorg Chem*, 1983, **30**, 359
- 5 Gy I Szasz, W Dietz, K Heinzinger, G Palinkas, and T Radnai, *Chem Phys Lett*, 1982, **92**, 338
- 6 D H Powell and G W Neilson, *J Phys Condens Matter*, 1990, **2**, 3871
- 7 W Dietz, W O Riede, and K Heinzinger, *Z Naturforsch*, 1982, **37a**, 1088
- 8 R D Broadbent, G W Neilson, and M Sandstrøm, *J Phys Condens Matter*, 1992, **4**, 1992
- 9 G J Herdman and G W Neilson, *J Phys Condens Matter*, 1992, **4**, 649
- 10 P V Kumar and B L Tembe, *J Chem Phys*, 1992, **97**, 4356
- 11 L Helm and A E Merbach, *Eur J Solid State Inorg Chem*, 1991, **28**, 245
- 12 C Cossy, A C Barnes, J E Enderby, and A E Merbach, *J Chem Phys*, 1989, **90**, 3254
- 13 N T Skipper and G W Neilson, *J Phys Condens Matter*, 1989, **1**, 4141
- 14 P Hemily, *Comptes Rendus*, 1953, **236**, 1579
- 15 N A Hewish, G W Neilson, and J E Enderby, *Nature*, 1982, **297**, 138
- 16 R D Broadbent and G W Neilson, *Chem Phys Lett*, 1991
- 17 P S Salmon, G W Neilson, and J E Enderby, *J Phys C Solid State Physics*, 1988, **21**, 1335
- 18 P S Salmon and G W Neilson, *J Phys Condens Matter*, 1989, **1**, 5291
- 19 L Curtis, J W Halley, and Z R Wang, *Phys Rev Lett*, 1992, **69**, 2435
- 20 D H Powell, A C Barnes, J E Enderby, G W Neilson, and P S Salmon, *Faraday Discuss Chem Soc*, 1988, **85**, 137
- 21 D H Powell, P M N Gullidge, G W Neilson, and M -C Bellissent-Funel, *Mol Phys*, 1990, **71**, 1107
- 22 S Cummings, J E Enderby, G W Neilson, J R Newsome, R A Howe, W S Howells, and A K Soper, *Nature*, 1980, **287**, 714
- 23 D H Powell, G W Neilson, and J E Enderby, *J Phys Condens Matter*, 1993, **5**, 5723
- 24 M Magini, G Licheri, G Paschina, G Piccaluga, and G Pinna, 'X-Ray Diffraction of Ions in Aqueous Solutions', 1988, CRC Press, Florida
- 25 M Sprik, M L Klein, and K Watanabe, *J Phys Chem*, 1990, **94**, 6483
- 26 L X Dang, J E Rice, J Caldwell, and P A Kollman, *J Am Chem Soc*, 1991, **113**, 2481